The Canadian Mineralogist
Vol. 44, pp. 177-188 (2006)

THE CRYSTAL STRUCTURE OF KIRKIITE, $Pb_{10}Bi_3As_3S_{19}$

EMIL MAKOVICKY, TONČI BALIĆ-ŽUNIĆ, LJILJANA KARANOVIĆ[¶] AND DEJAN POLETI[†]

Geological Institute, University of Copenhagen, Øster Voldgade 10, DK–1350 Copenhagen K, Denmark

ABSTRACT

The crystal structure of kirkiite has been solved using single-crystal data (Mo$K\alpha$ X-ray diffraction, CCD area detector) to the conventional R-factor R_1 = 0.069. It crystallizes in space group $P2_1/m$, with a 8.621(4), b 26.03(1), c 8.810(4) Å, β 119.21(1)° and Z = 2. A crystal-structure determination and chemical analysis resulted in comparable formulae, $Pb_{10}Bi_{2.16}As_{3.84}S_{19}$ and $Pb_{10.08}Bi_{2.55}Sb_{0.13}As_{2.91}S_{19}$, respectively, which are close to the ideal formula $Pb_{10}Bi_3As_3S_{19}$. The crystal lattice shows a pseudohexagonal symmetry, which is the cause of common twinning in this mineral. The main twin-law has $(20\bar{1})$ as a twin plane, with [100] as the twin axis, owing to the orthorhombic distortion of the pseudohexagonal lattice in accordance with the alignment of lone-electron-pair micelles in rows parallel to (001). The twin mechanism explains the formation of observed twin-lamellae with $(20\bar{1})$ as a contact plane. The crystal structure of kirkiite can be described as (010) slabs of octahedra, three octahedra thick and related mutually by a reflection plane situated in the intervening prismatic layer. In another interpretation, it is composed of slabs based on a transitional PbS–SnS archetype, with tightly bonded layers parallel to (083) of kirkiite; the slabs are unit-cell-twinned on (010) reflection planes. The structure contains one split As position, and two additional sites that could accommodate both As and Bi. The As,Bi distribution over these two sites is determined by the trapezoidal distortion of the half-octahedral coordination environment inside the tightly bonded double layers of the PbS–SnS archetype slabs. Owing to the stoichiometry requirements in this structure, Bi must also substitute for 1/11 of the Pb sites. Bond-valence calculations and the volumes of coordination polyhedra show it to be ordered in two of the Pb sites. Kirkiite and jordanite $Pb_{28}As_{12}S_{46}$ are a pair of homologues. The general formula of a potential homologous series is $Pb_{8N-4}Me^{3+}{}_{12}S_{8N+14}$.

Keywords: kirkiite, crystal structure, sulfosalt, jordanite homologous series.

SOMMAIRE

Nous avons résolu la structure cristalline de la kirkiite avec données obtenues sur monocristal avec un rayonnement Mo$K\alpha$ et un détecteur à aire de type CCD, jusqu'à un résidu R_1 de 0.069. Elle cristallise dans le groupe spatial $P2_1/m$, avec a 8.621(4), b 26.03(1), c 8.810(4) Å, β 119.21(1)° et Z = 2. L'ébauche de la structure et une analyse chimique mènent à des formules comparables, $Pb_{10}Bi_{2.16}As_{3.84}S_{19}$ et $Pb_{10.08}Bi_{2.55}Sb_{0.13}As_{2.91}S_{19}$, respectivement, et comparables à la formule idéale, $Pb_{10}Bi_3As_3S_{19}$. Le réseau possède une symétrie pseudohexagonale, qui est la cause du développement de macles dans ce minéral. La loi de macle principale possède $(20\bar{1})$ comme plan de macle, et [100] est l'axe de la macle, à cause de la distorsion orthorhombique de la maille pseudohexagonale, en accord avec l'alignement des micelles des paires d'électrons isolés en rangées parallèles à (001). Le mécanisme du maclage rend compte de la formation des lamelles de macle observées ayant $(20\bar{1})$ comme plan de contact. La structure de la kirkiite peut se décrire en termes de plaques (010) d'octaèdres d'une épaisseur de trois octaèdres de chaque côté d'un plan de réflexion situé dans le niveau prismatique intercalé. Selon une autre interprétation, la structure est faite de plaques fondées sur l'archétype PbS–SnS transitionnel, avec des couches fortement rattachées parallèles à (083) de la kirkiite; ces plaques sont maclées sur une échelle de la maille élémentaire avec (010) comme plan de réflexion. La structure contient une position As partagée, et deux sites additionnels qui peuvent accommoder à la fois As et Bi. La distribution de As et Bi sur ces deux sites dépend de la distorsion trapézoïdale du milieu de coordinence semi-octaédrique à l'intérieur des couches doubles fortement rattachées des plaques de l'archétype PbS–SnS. Vues les exigeances de la stoéchiométrie dans cette structure, le Bi doit aussi remplacer 1/11 des sites Pb. D'après les calculs des valences de liaison et du volume des polyèdres de coordinence, l'As serait incorporé à deux des sites Pb. La kirkiite et la jordanite $Pb_{28}As_{12}S_{46}$ définissent une paire d'homologues. La formule générale d'une séries d'homologues potentielle serait $Pb_{8N-4}Me^{3+}{}_{12}S_{8N+14}$.

(Traduit par la Rédaction)

Mots-clés: kirkiite, structure cristalline, sulfosel, série d'homologues de la jordanite.

[§] *E-mail address*: emilm@geol.ku.dk

[¶] On leave from the Faculty of Mining and Geology, Đušina 7, 11000 Belgrade. Serbia and Montenegro.

[†] On leave from the Faculty of Technology and Metallurgy, Karnegijeva 4, 11000 Belgrade, Serbia and Montenegro.

INTRODUCTION

Kirkiite was first discovered in the lead–zinc deposit of Aghios Philippos, near Kirki, in Thrace, Greece. Optical properties, X-ray powder and single-crystal diffraction data, as well as results of electron-microprobe investigations, were reported by Moëlo *et al.* (1985). The first occurrence of a Se-bearing variety of kirkiite, from the fumarole of La Fossa crater on Vulcano Island, Italy, was described by Borodaev *et al.* (1998). Here, we report on the crystal structure of kirkiite from the type locality.

BACKGROUND INFORMATION

The type kirkiite from Kirki, of composition $Pb_{10.08}Bi_{2.55}Sb_{0.13}As_{2.91}S_{19}$, was found to be polysynthetically twinned in reflected light. Observable twin-lamellae assume only one orientation and are very fine. Single-crystal X-ray photographs perfectly simulate a hexagonal symmetry, the product of this twinning, with *a* 8.69(5) and *c* 26.06(10) Å, the systematic extinction simulating the space group $P6_322$. Moëlo *et al.* (1985) described a two-tier system of subcells, which can easily be tied to the submotifs of the structure determined in the present work. This assignment has to a large extent already been done by Moëlo *et al.* (1985), who also noticed the similarities with the reciprocal lattice of jordanite (Wuensch & Nowacki 1966). Moëlo *et al.* (1985) and Makovicky (1989) also established the homology of kirkiite to jordanite, $Pb_{28}As_{12}S_{46}$ (Ito & Nowacki 1974). The true symmetry of kirkiite was suggested to be $P2_1$, $P2_1/m$ or $C222_1$.

Selenian kirkiite from Vulcano, $Pb_{10}As_{3.4}Bi_{2.6}S_{18.6}Se_{0.4}$ was studied by electron micro-diffraction (Borodaev *et al.* 1998). Only one incidence of polysynthetic twinning was observed on the tiny pseudohexagonal crystals of this product of sublimation. Borodaev *et al.* (1998) distinguished (a) monoclinic, strongly pseudohexagonal crystals with *a* 8.4(6), *b* 7.8(6), *c* 26.0(1) Å, β 118(1)° and space group given as $P2_1$, (b) the same with diffuse streaks for those reciprocal lattice rows that have $h = 2n + 1$ and are parallel to c^*, and (c) a rare $B2/m$, Bm or $B2$ case with a doubled *c*-value. The results from their powder-diffraction refinement, *a* 8.47(5), *b* 7.84(5), *c* 25.97(1) Å, β 118.03(1)° (space group $P2_1/m$), are at variance with the present work.

EXPERIMENTAL

The current structure-determination was performed on a crystal fragment from the type specimen. The chemical formula of the compound, determined by electron-microprobe analysis, gives Pb 59.4, Sb 0.5, Bi 15.2, As 6.2, S 17.4, total 98.7 wt.%, corresponding to $Pb_{10.8}Bi_{2.55}Sb_{0.13}As_{2.91}S_{19}$, on the basis of S = 19 atoms or, ideally, $Pb_{10}Bi_3As_3S_{19}$ (Moëlo *et al.* 1985).

An irregular grey fragment of approximate dimensions 0.07 × 0.07 × 0.05 mm was used for the crystal-structure analysis. Room-temperature data (298 K) were collected on a Bruker–AXS four-circle diffractometer equipped with SMART 1000 area detector (6.25 × 6.25 cm active area, resolution 81.92 pixels cm^{-1}) and a flat graphite monochromator, using Mo*K*α radiation from a fine-focus sealed X-ray tube. The sample-to-detector distance was 3.85 cm. A total of 1050 exposures (frame width 0.3°, time 120 s) were collected.

This resulted in 6339 reflections ($5.30 < 2\theta < 46.52°$) with Miller indices in the range $-9 < h < 6$, $-28 < k < 16$ and $-6 < l < 9$, of which 2535 are considered unique and 887 are stronger than 2σ(I). Final unit-cell parameters were determined using 496 strong reflections with I > 10σ(I). The software SMART was used for cell-parameter determination and data collection, SAINT for integration of intensities, Lorentz–polarization correction and calculation of the final unit-cell parameters. Attempts to carry out an empirical absorption-correction did not improve the R_{int} factor significantly, and suggested relatively small differences between the minimum and maximum transmission. Furthermore, it was possible to obtain a better refinement with the uncorrected data, and the absorption correction was abandoned. The problems are probably caused by an uneven distribution of the twin components in the crystal. Data on the crystal and the measurements are given in Table 1.

SOLUTION OF THE STRUCTURE

The crystal lattice of kirkiite has a distinctly pseudohexagonal character. Careful refinement of these cell parameters resulted in a monoclinic unit-cell with close but clearly different lengths of *a* and *c* axes, and

TABLE 1. CRYSTAL DATA AND DETAILS OF THE STRUCTURE REFINEMENT OF KIRKIITE

Empirical formula (from diffraction)	$Pb_{10}Bi_{2.16}As_{3.84}S_{19}$
Formula weight	3420.21
Crystal system, space group (No.)	Monoclinic, $P\,2_1/m$ (11)
a (Å)	8.621(4)
b (Å)	26.03(1)
c (Å)	8.810(4)
β (°)	119.21(1)
V ($Å^3$)	1726(1)
Z	2
D_x ($Mg\,m^{-3}$)	6.580
μ (mm^{-1})	64.473
F(000)	2860
Range for data collection, θ (°)	2.65 – 23.26
Limiting indices	$-9 \le h \le 6$, $-28 \le k \le 16$, $-6 \le l \le 9$
Reflections collected / unique	6339 / 2535 ($R_{int} = 0.1456$)
Reflections unique observed [I > 2σ(I)]	887
Data / restraints / parameters	2535 / 0 / 113
Goodness-of-fit, *S*	0.852
R indices [$I > 2\sigma(I)$]	$R_1 = 0.0690$, $wR_2 = 0.1427$ [‡]
R indices (all data)	$R_1 = 0.2070$, $wR_2 = 0.1821$

[‡] $w = 1/[\sigma^2(F_o^2) + (0.0610P)^2]$, where $P = (F_o^2 + 2\,F_c^2)/3$.

a β angle of 119.20° (Table 1). No general systematic extinctions were observed, indicating a primitive lattice. However, all reflections with $h + l \neq 2n$ are significantly weaker, suggesting a pseudo-*B* centering of the lattice. Among the special extinction conditions, only $0k0$, $k = 2n$ rule was observed, and in accordance with this finding, $P2_1/m$ was assumed as the most probable space-group. A transformation of the above lattice-basis by the matrix $1\ 0\ 0/1\ 0\ 2/\ 0\ \bar{1}\ 0$ produces a close-to-orthorhombic *C*-lattice with the three angles 90.0, 90.0 and 89.91. When the monoclinic structure was solved and refined, the solution was attempted also in the orthorhombic system, space group *Cmcm* based on the transformed lattice, and in the triclinic system, space group $P\bar{1}$, with the monoclinic lattice as a base. Both solutions produced results duplicating features from the monoclinic model. The orthorhombic one had features of a twinned structure in accordance with the twin law most probable for kirkiite, whereas the triclinic one contained full "pseudo"-symmetry elements of the monoclinic solution. The R-factors were also higher than for the monoclinic solution.

The structure was solved by direct methods (SHELXS97, Sheldrick 1997a), which revealed positions of all metal and semimetal atoms. The sulfur atoms were found in difference-Fourier maps during the subsequent refinements of the structure by full-matrix least-squares on F^2 (SHELXL97, Sheldrick 1997b). At the beginning of the refinement, all cation positions were defined as Pb, because there were no clear differences between maxima found by direct methods. High displacement-factors indicated occupancy by a lighter element for two positions; they were attributed to As, leading to improved *R* factors. For the As position, which at first was considered to be on a symmetry plane (As3), a very elongate displacement ellipsoid and uncharacteristically short As–S distances suggested a splitting over two symmetrically equivalent positions close to the symmetry plane, with half-occupancy each. Pseudosymmetry of the crystal lattice and consistently high residual factors suggested the presence of pseudomerohedral twinning. Introduction of twinning into the refinement improved *R*-values significantly.

Owing to the pseudohexagonal nature of the crystal lattice, there are three different possible patterns of pseudomerohedral twinning, which are discussed later in the description of the structure. The one that is metrically most suitable gave also the best *R*-factors and the highest content of the second twin component (40%), and was therefore used for the final results. As the structural model revealed three positions with coordinations characteristic for As or Bi, but not for Pb, a possibility of Bi-for-As substitution at these positions was investigated. Attempts to refine them as mixed positions were successful only for the Bi1 position, which at the end of the refinement displays 42% As occupancy. The other two positions refined as pure As. The fractional coordinates of Bi and As were kept free, whereas the atom-displacement factor of As1 (sharing the position with Bi1) was constrained to be equal to that of As2, which has the same type of environment. Analysis of coordination characteristics suggested the Pb4 and Pb6 positions as hosts for additional Bi in the structure. The occupancies of Pb and Bi at these positions were fixed using the results of coordination analysis, and no refinement of their occupancies was attempted, because of a negligible difference in the scattering powers of the two elements. All Pb and (Pb,Bi) positions were refined with anisotropic displacement factors, whereas other cation positions were kept isotropic, because attempts of anisotropic refinement proved unsuccessful. The largest final correlation-factors (over 0.7) were found between

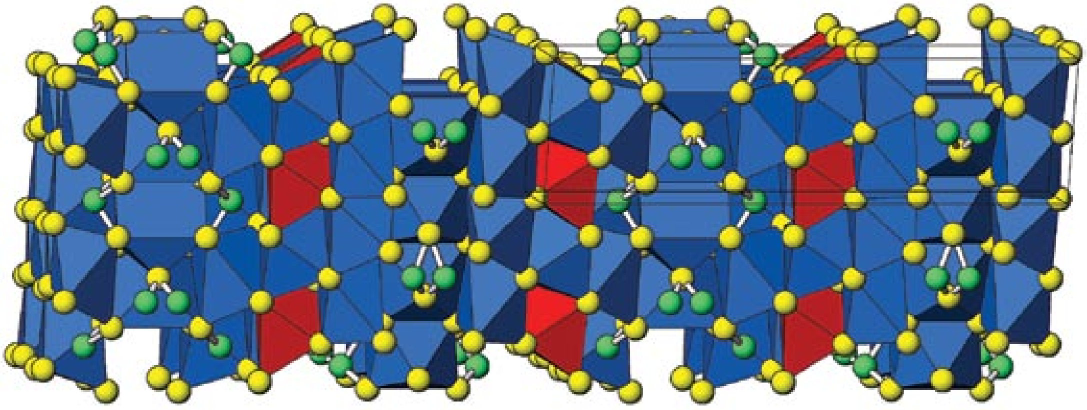

FIG. 1. The crystal structure of kirkiite, $Pb_{10}Bi_3As_3S_{19}$, in polyhedron description. The mixed (Bi1,As1) polyhedron is red, Pb and (Pb,Bi) coordination octahedra and prisms are blue, arsenic is green (note the split As3 position), and S is yellow. Triple-octahedron slabs (010) are separated by layers of capped trigonal coordination prisms.

atom-displacement factors of heavy atoms and between coordinates of As1 and Bi1. The final coordinates and displacement parameters of the atoms are presented in Tables 2 and 3, whereas the bond lengths and polyhedron characteristics are listed in Tables 4 and 5. A table of structure factors has been sent to the Depository of Unpublished Data, CISTI, National Research Council of Canada, Ottawa, Ontario K1A 0S2.

The highest residual maximum and minimum in the last difference-Fourier map were 3.43 e Å^{-3} (0.97 Å from Bi1 and As1) and –3.94 e Å^{-3} (0.70 Å from S11).

MODULAR DESCRIPTION OF THE STRUCTURE

The crystal structure of kirkiite and that of its homologue jordanite can be described in two ways. Firstly, it can be considered as a stacking sequence of (distorted) layers of octahedra and trigonal prismatic layers, which share sulfur atoms along their boundaries; they are parallel to (010) of the monoclinic unit-cell (Fig. 1). Stacks of three layers of octahedra alternate with prismatic layers in kirkiite (Figs. 2a–c), whereas stacks of four such layers are present in the crystal structure of jordanite. The slabs of octahedra were characterized as (111) layers of the PbS archetype by Moëlo *et al.* (1985) and Makovicky (1989). Stacks of octahedra surrounding a layer of trigonal prisms are related by a mirror plane coincident with the median plane of the latter. Secondly, it can be considered in terms of (111) slabs of distorted PbS archetype or (210) slabs of SnS archetype, three and four SnS or PbS subcells broad for kirkiite (Fig. 3) and for jordanite, respectively; these are mirror-twinned on (010) of the lattice of these respective structures, with the tightly bonded double-layers and intervening lone-electron-pair micelles present in both these structures. These double layers are parallel to the *a* axis in kirkiite and *c* axis in jordanite and are diagonal to the layers of octahedra defined above.

TABLE 2. FRACTIONAL COORDINATES, EQUIVALENT DISPLACEMENT AND OCCUPATION PARAMETERS OF ATOMS IN KIRKIITE

Atom	x	y	z	U_{eq} (Å^2)	Occupancy (%)
Pb1	0.7400(9)	0.0026(1)	0.2340(6)	0.033(1)	1
Pb2	0.5833(9)	0.1225(1)	0.4235(7)	0.034(1)	1
Pb3	0.0702(8)	0.12613(9)	0.9000(6)	0.027(1)	1
Pb4	0.5736(8)	0.12606(9)	0.9023(6)	0.029(1)	0.75
Bi4	0.5736(8)	0.12606(9)	0.9023(6)	0.029(1)	0.25
Pb5	0.934(1)	0.2500	0.1162(8)	0.045(2)	1
Pb6	0.906(1)	0.2500	0.5696(9)	0.029(2)	0.5
Bi6	0.906(1)	0.2500	0.5696(9)	0.029(2)	0.5
Pb7	0.406(1)	0.2500	0.567(1)	0.038(2)	1
Bi1	0.241(1)	0.0021(3)	0.239(1)	0.010(2)	0.58(2)
As1	0.277(5)	-0.004(1)	0.259(5)	0.014(2)	0.42(2)
As2	0.074(2)	0.1200(2)	0.416(1)	0.014(2)	1
As3	0.408(3)	0.2805(5)	0.073(2)	0.019(3)	0.50
S1	0.412(4)	0.0621(5)	0.044(2)	0.012(5)	1
S2	0.868(5)	0.0557(8)	0.016(3)	0.046(7)	1
S3	0.469(4)	0.0548(6)	0.623(3)	0.019(6)	1
S4	0.897(4)	0.0539(7)	0.615(3)	0.025(6)	1
S5	0.830(4)	0.1649(8)	0.292(4)	0.032(7)	1
S6	0.213(3)	0.1649(7)	0.281(4)	0.023(6)	1
S7	0.739(6)	0.1811(7)	0.719(3)	0.037(6)	1
S8	0.207(4)	0.1638(7)	0.669(3)	0.033(5)	1
S9	0.548(4)	0.2500	0.944(4)	0.014(8)	1
S10	0.12(1)	0.2500	0.930(8)	0.09(2)	1
S11	0.548(7)	0.2500	0.343(4)	0.036(7)	1

U_{eq} is defined as 1/3 of the trace of the orthogonalized U_{ij} tensor.

TABLE 3. ANISOTROPIC DISPLACEMENT PARAMETERS, U_{ij} (Å^2), FOR KIRKIITE

Site	U_{11}	U_{22}	U_{33}	U_{23}	U_{13}	U_{12}
Pb1	0.032(4)	0.025(2)	0.049(3)	0.003(2)	0.025(3)	0.003(2)
Pb2	0.039(4)	0.029(2)	0.043(3)	-0.002(1)	0.026(3)	0.004(3)
Pb3	0.014(3)	0.023(2)	0.038(4)	0.001(2)	0.006(3)	0.003(2)
[Pb,Bi]4	0.017(3)	0.021(2)	0.040(4)	0.003(2)	0.007(3)	-0.003(2)
Pb5	0.056(6)	0.026(2)	0.068(4)	0.000	0.042(6)	0.000
[Pb,Bi]6	0.009(4)	0.027(3)	0.027(5)	0.000	-0.011(4)	0.000
Pb7	0.011(5)	0.034(3)	0.043(6)	0.000	-0.008(4)	0.000

The stack of double layers in both structures approximates an array that is transitional between the PbS and SnS archetypes; in kirkiite, the average angle between $(100)_{PbS}$ and $[100]_{PbS}$ is 17.4° (or 14.3° without Pb3 and Pb4). Trapezoidal distortion of the cation coordination-polyhedron is strongest for the rows Pb2–As2, intermediate for Pb1–(Bi,As)1, and weak for Pb3–Pb4 (Fig. 4).

A description of kirkiite and jordanite as composed of SnS- or PbS-like layers twinned on $(210)_{SnS}$, *i.e.*, on $(111)_{PbS}$, by mirror reflection across the boundary layer of capped trigonal prisms, offers a completely new view of this family. There is a pronounced analogy in the distribution of sites occupied by trivalent metalloids in these two structures.

In kirkiite (N = 3), the slabs are three, and in jordanite (N = 4), four coordination pyramids across. Thus, the homologous pair kirkiite–jordanite leads to a general formula $Pb_{8N-4}As_{12}S_{8N+14}$ for the potential kirkiite homologous series, and to the prediction of both lower and higher members of the series: homologue N = 1, with a model composition $Pb_4As_{12}S_{22}$, homologue N = 2, with a composition $Pb_{12}As_{12}S_{30}$, and N = 5, with a formula $Pb_{36}As_{12}S_{54}$; a part of the "As" in these formulae might stand for Bi or even Sb.

COORDINATION POLYHEDRA

The distribution of cation polyhedra in a tightly bonded diagonal double layer and their disposition over the (010) layers of octahedra and prisms exert a substantial influence on their coordination properties.

The central portions of the diagonal double layer are assumed by the skewed distorted coordination octahedra of Bi1 and Pb1 (Fig. 2a). Both octahedra have a 3 + 3 coordination. The ratio of short bond that stretches across the tightly bonded diagonal double layer to the opposing long distance situated across the layer-like lone-electron-pair micelle is 2.48 to 3.27 Å for Bi1, in agreement with its mixed occupancy (58% Bi and 42% As), and 2.72 to 3.23 Å for Pb1; the angle between the "horizontal" S–*Me*–S direction and the perpendicular MeS_4 plane is 164° for both. Distortion of these coordination polyhedra can be appreciated from their volume-based distortion coefficients (Makovicky & Balić-Žunić 1998): ν(Pb1) = 0.065, ν(Bi1) = 0.123. The apparent overbonding for Bi1 and underbonding for As1 (Table 5) result from the fact that their S ligands are the average S positions in this statistically occupied octahedron.

Proceeding toward the marginal parts of the double layer, Pb2 (Fig. 2b) has a similarly distorted octahedron (ν = 0.074) (paired with As2 that is situated along the direction of the *a* axis), with the ratio of distances equal to 2.74 *versus* 3.32 Å. The other Pb2–S distances are typical for Pb (2.98–3.08 Å; this is close to 2.97 Å, *i.e.*, the sum of crystal radii of Pb and S). The shape of the associated As2 polyhedron is influenced by the necessity of adjusting to the array of large cation polyhedra; it has three typical short distances (2.18–2.37 Å) opposed by long As–S contacts (3.31–3.50 Å). The short distances are oriented toward the empty triangular space situated in the adjacent layer of prisms. The As–S distance across the barycenter of the lone-electron-pair micelle is 3.50 Å.

The Pb3 and Pb4 atoms, alternating with the previous ones in the marginal portions of the stack of octahedra, have a fairly uniform environment (Fig. 2b). The above ratio of bond lengths is 2.90:3.13 Å and 2.86:3.21 Å, respectively. The Pb–S distances pointing toward the layer of prisms are the longest ones for the mixed (Pb,Bi) site, denoted as Pb4; the opposite is true for Pb3. Both atoms have an additional Pb–S distance toward S atoms on the adjacent mirror plane, equal to 3.13 and 3.27 Å, (*i.e.*, their coordination polyhedra can also be described as monocapped trigonal prisms rotated 90° with respect to those of Pb5–Pb7, or as "split octahedra").

The interlayer of trigonal prisms (Fig. 2c) contains Pb5, Pb6 and Pb7 as well as As3. Both the lead sites Pb5 and Pb7, and the mixed (Pb,Bi) position denoted as Pb6, have a bicapped trigonal prismatic coordination, with one set of central cation-to-corner ligand distances distinctly larger than the rest, and with prism caps invariably exhibiting the shortest Pb–S distance. The split As3 position has short As–S distances (As–S9 = 2.19, As–S10 = 2.15, and As–S11 = 2.22 Å) to the three S atoms on the mirror plane. The statistically occupied As3–As3' positions are situated about the median plane of a trigonal prism formed by S5, S6 and S8 (S–As in the range 3.34–3.47 Å), *i.e.*, a tricapped trigonal prism with very low caps. Based on the mixed cation positions, kirkiite with maximum As contents could reach the composition $Pb_{10}BiAs_5S_{19}$; the composition with a minimum amount of arsenic, $Pb_{10}Bi_5AsS_{19}$ seems less probable. None of these was observed in nature or in the syntheses by Walia & Chang (1973).

TWINNING AND DISORDER

The pseudotrigonal character of kirkiite and its pseudo-orthorhombic centered lattice determined in the present study enable us to suggest structural mechanisms for both the observed twinning of kirkiite and for the disorder phenomena observed by Borodaev *et al.* (1998).

In the layers of trigonal prisms as well as in the layers of octahedra, the principal distortion away from the trigonal geometry is the trace of the lone-electron-pair micelle of the distorted PbS-like structures. These micelles are ordered in stripes parallel to [100]. Therefore, the periods [001] and [101] of the kirkiite lattice differ very little (8.81 and 8.82 Å, respectively), but they are substantially longer than the [100] period, which is equal to 8.62 Å. All these directions would be identical in the idealized trigonal motif. On the structural level, in all layers of atoms parallel to (010), pseudo-mirror planes are present with traces parallel to [102]. Thus, the principal twin-law expected is either (001) as the twin plane and [102] as twin axis, or $(20\bar{1})$ as the twin plane and [100] as twin axis. These modes of twinning will preserve the orientation of the pronounced lone-electron-pair micelles, *i.e.,* such a preservation will be a preferred mechanism of twinning.

The simplest model of twinning is based on an OD mechanism (order–disorder mechanism for layer polytypes, Ďurovič 2004) in the (010) layers of octahedra or trigonal prisms (Fig. 2). The row [100] of alternating Pb6 and Pb7 polyhedra in the prismatic layer (Fig. 2c) is attached laterally to the row of alternating Pb5 and As3 polyhedra. Both of the configurations As3–Pb7–Pb6 and Pb5–Pb6–Pb7 are highly symmetrical, their Pb7-based and Pb6-based halves being near-reflection images of each other. Therefore, if a mixed atom Pb6' is mistakenly implanted on the "wrong" side of such a cation triplet, at the site where pure lead Pb7 should occur and, as a consequence, if a shift of the Pb6–Pb7 sequence by (1/2)*c* takes place, such an error meets with only a minor penalty in energy within the individual (010) layer. The vector Pb5–Pb6 that defines the [001] direction will be reflected in the [101] direction of the original cell, producing the above-described twinning. The same scheme is also valid for both the first and the second layers of octahedra, causing the sites Pb3 and Pb4, and the sites Bi1 and Pb1 to be interchanged, in the tightly bonded strips (Figs. 2b, a). However, when proceeding across the stack of [010] layers of octahedra, the last layer of octahedra before the next (010) layer of prisms presents a different situation. Here, the shifts involve interchanging Pb2 with As2, which alters the As2–As2 relationship across the intervening Pb6–Pb7 column. This is not the OD relationship seen in the previous

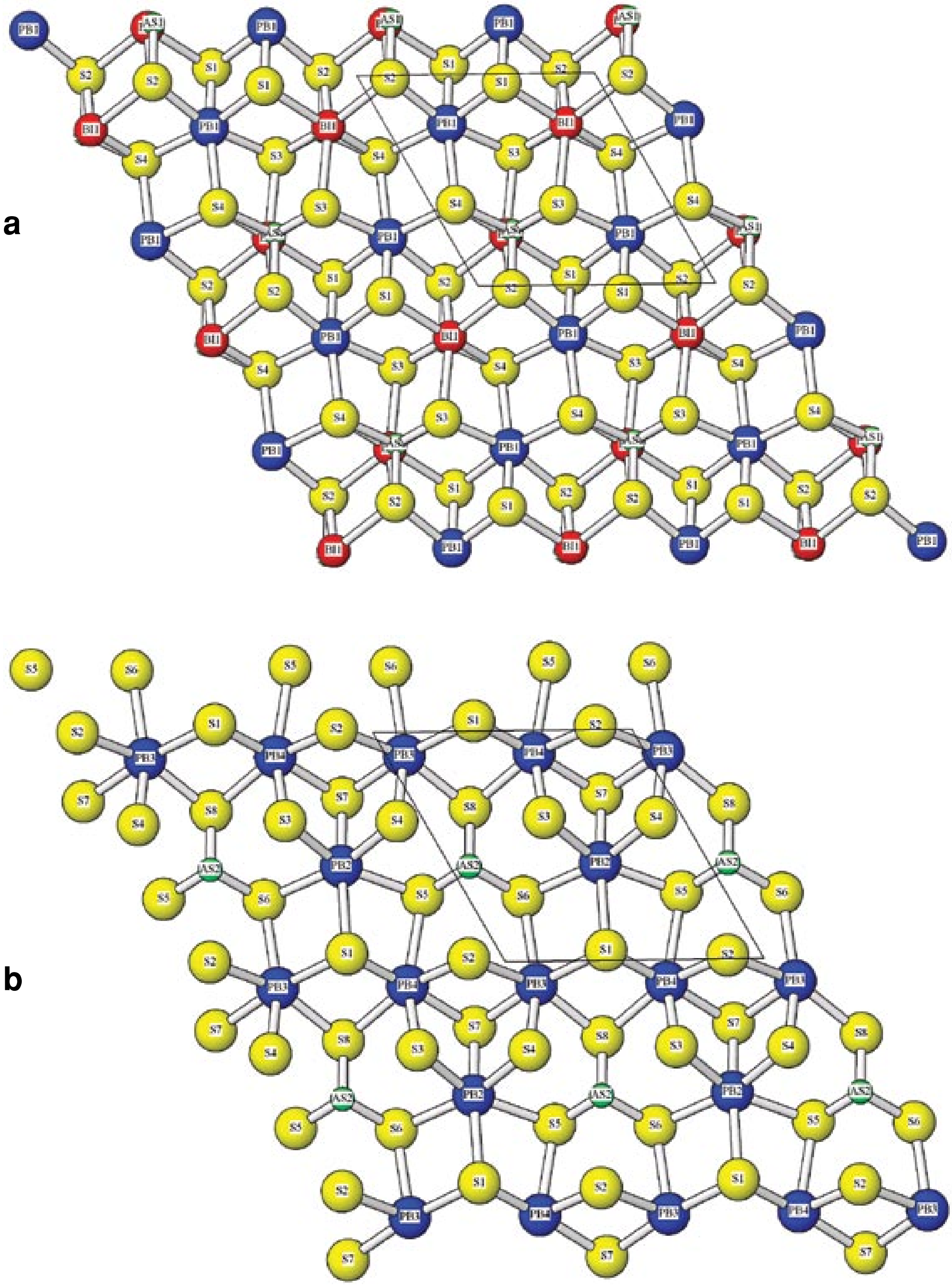
a
PB1
AS1
BI1
S1
S2
S3
S4
b
PB2
PB3
PB4
AS2
S1
S2
S3
S4
S5
S6
S7
S8

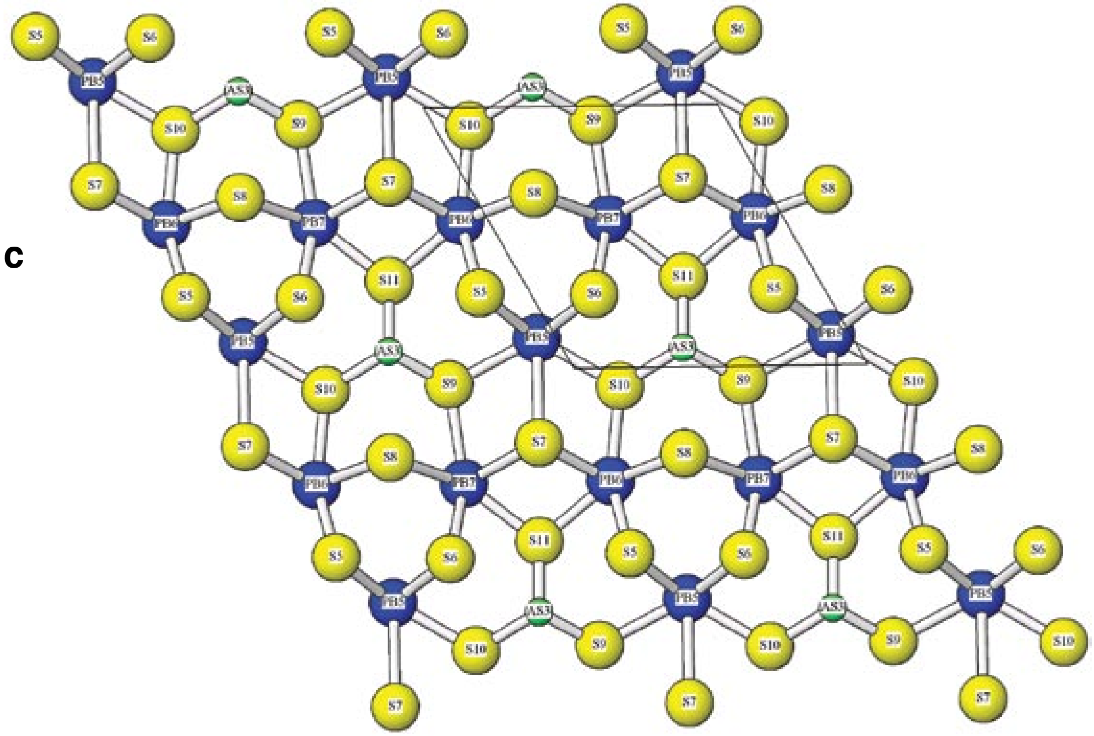

FIG. 2. Component layers of polyhedra from the crystal structure of kirkiite: (a) the layer of coordination octahedra in the central portion of the slab of octahedra at $y = 0.5$, (b) the layer of octahedra at the margins of the slab of octahedra ($y \approx 0.325$), and (c) the layer of capped trigonal coordination prisms at $y = 0.25$. Consecutive layers share sulfur atoms. The *a* axis is oriented to the left, *c* axis downward.

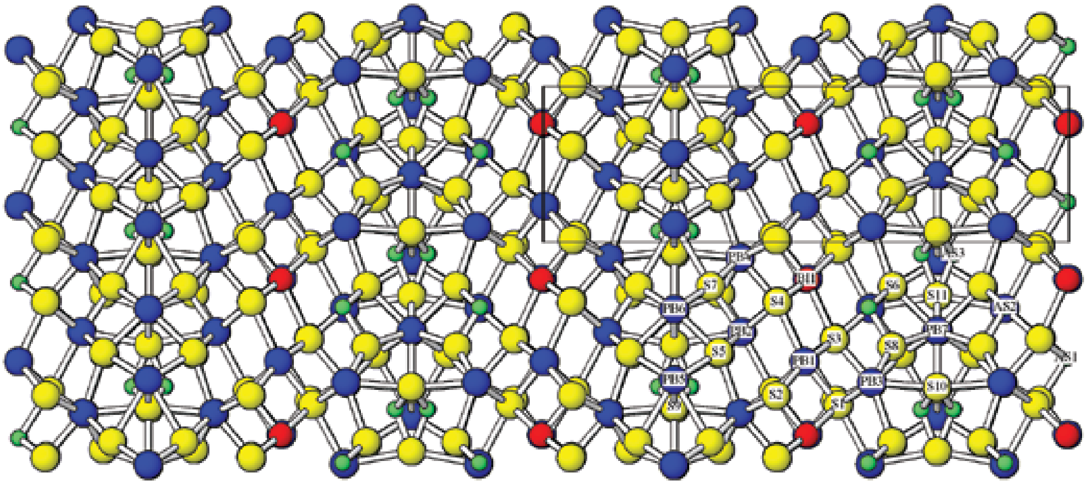

FIG. 3. Projection of the crystal structure of kirkiite along [100]. The *b* axis points to the right, d_{001} downward. Note the transitional PbS–SnS character of the slabs of "octahedra" and the complex, mirror-symmetric layers of prisms at $y = 0.25$ and 0.75, with a split As3 position.

TABLE 4. THE STATE OF COORDINATION OF CATIONS IN KIRKIITE

Atom **Pb1**, CN: 6, bonded to:

	S1	**S1**	**S2**	**S3**	**S4**	**S4**
S1	**2.724(15)**	84.6(9)	82.8(8)	86.9(7)	92.0(7)	164.4(7)
S1	3.809(31)	**2.929(25)**	86.8(8)	84.0(7)	169.9(7)	100.0(7)
S2	3.777(38)	4.061(58)	**2.981(39)**	166.8(8)	83.3(8)	112.2(8)
S3	3.977(42)	3.998(25)	5.987(52)	**3.047(35)**	105.4(7)	78.8(7)
S4	4.203(33)	6.014(38)	4.048(29)	4.897(52)	**3.109(30)**	85.8(10)
S4	5.902(27)	4.723(27)	5.160(45)	3.988(32)	4.318(43)	**3.232(24)**

Atom **Pb2**, CN: 6, bonded to:

	S7	**S3**	**S4**	**S6**	**S5**	**S1**
S7	**2.738(22)**	85.3(9)	84.7(9)	96.9(9)	92.9(10)	173.0(9)
S3	3.876(37)	**2.976(31)**	77.4(7)	82.8(7)	157.3(8)	101.6(7)
S4	3.857(40)	3.725(52)	**2.983(25)**	159.9(8)	80.0(8)	97.0(7)
S6	4.307(39)	3.959(29)	5.903(35)	**3.012(24)**	119.8(8)	83.9(7)
S5	4.222(58)	5.938(51)	3.896(37)	5.273(49)	**3.080(41)**	80.8(7)
S1	6.046(27)	4.884(37)	4.723(27)	4.238(41)	4.152(34)	**3.319(16)**

Atom **Pb3**, CN: 7, bonded to:

	S7	**S4**	**S8**	**S2**	**S1**	**S6**	**S10**
S7	**2.881(39)**	83.7(9)	94.3(9)	84.8(9)	172.2(9)	101.5(9)	67.0(13)
S4	3.857(40)	**2.900(21)**	80.2(8)	76.2(8)	89.5(7)	154.9(8)	134.9(13)
S8	4.291(65)	3.783(38)	**2.973(35)**	156.4(8)	80.8(7)	123.3(7)	69.2(13)
S2	3.988(30)	3.662(48)	5.876(52)	**3.030(39)**	97.2(8)	79.8(8)	130.6(13)
S1	5.937(48)	4.203(33)	3.918(25)	4.578(57)	**3.070(28)**	86.3(7)	116.2(12)
S6	4.652(35)	5.882(36)	5.367(49)	3.950(32)	4.238(41)	**3.125(32)**	68.0(12)
S10	3.398(71)	5.680(31)	3.541(76)	5.704(53)	5.364(37)	3.565(64)	**3.248(9)**

Atom **Pb4**, CN: 7, bonded to:

	S1	**S3**	**S2**	**S8**	**S7**	**S5**	**S9**
S1	**2.823(29)**	88.9(7)	90.7(8)	85.0(7)	171.8(9)	86.8(7)	117.2(7)
S3	3.977(42)	**2.854(22)**	75.0(8)	80.6(8)	83.1(9)	152.9(8)	136.8(8)
S2	4.061(58)	3.492(34)	**2.884(34)**	155.3(8)	85.5(9)	78.4(8)	133.2(8)
S8	3.918(25)	3.770(40)	5.722(43)	**2.973(27)**	95.4(9)	125.5(8)	69.1(7)
S7	5.798(52)	3.876(37)	3.988(30)	4.411(64)	**2.990(45)**	99.5(9)	70.3(8)
S5	4.152(34)	5.894(35)	3.857(43)	5.496(33)	4.734(49)	**3.208(28)**	67.5(8)
S9	5.205(22)	5.693(25)	5.648(31)	3.549(29)	3.612(57)	3.598(32)	**3.267(7)**

Atom **Pb5**, CN: 8, bonded to:

	S10	**S9**	**S6**	**S6**	**S5**	**S5**	**S7**	**S7**
S10	**2.803(97)**	122.2(15)	74.7(14)	74.7(14)	133.4(15)	133.4(15)	63.5(14)	63.5(14)
S9	5.00(101)	**2.909(32)**	132.9(8)	132.9(8)	73.8(8)	73.8(8)	67.3(8)	67.3(8)
S6	3.565(64)	5.475(35)	**3.064(21)**	92.6(10)	66.1(8)	129.5(8)	136.0(8)	89.2(8)
S6	3.565(64)	5.475(35)	4.431(26)	**3.064(21)**	129.5(8)	66.1(8)	89.2(8)	136.0(8)
S5	5.402(95)	3.598(32)	3.350(50)	5.555(37)	**3.078(34)**	92.1(12)	138.3(8)	91.0(8)
S5	5.402(95)	3.598(32)	5.555(37)	3.350(50)	4.431(30)	**3.078(34)**	91.0(8)	138.3(8)
S7	3.398(71)	3.612(57)	6.127(31)	4.652(35)	6.189(41)	4.734(49)	**3.542(23)**	60.8(11)
S7	3.398(71)	3.612(57)	4.652(35)	6.127(31)	4.734(49)	6.189(41)	3.588(26)	**3.542(23)**

Atom **Pb6**, CN: 8, bonded to:

	S11	**S10**	**S7**	**S7**	**S5**	**S5**	**S8**	**S8**
S11	**2.738(47)**	135.8(16)	72.9(11)	72.9(11)	72.4(10)	72.4(10)	132.2(10)	132.2(10)
S10	5.120(65)	**2.788(59)**	72.1(15)	72.1(15)	131.3(15)	131.3(15)	71.9(14)	71.9(14)
S7	3.403(34)	3.398(71)	**2.979(43)**	74.1(14)	144.2(9)	87.5(9)	143.2(9)	87.7(9)
S7	3.403(34)	3.398(71)	3.588(26)	**2.979(43)**	87.5(9)	144.2(9)	87.7(9)	143.2(9)
S5	3.477(59)	5.388(65)	5.807(46)	4.222(58)	**3.123(29)**	90.4(11)	63.3(8)	122.8(8)
S5	3.477(59)	5.388(65)	4.222(58)	5.807(46)	4.431(30)	**3.123(29)**	122.8(8)	63.3(8)
S8	5.444(55)	3.541(76)	5.875(51)	4.291(65)	3.326(33)	5.563(30)	**3.212(27)**	88.6(10)
S8	5.444(55)	3.541(76)	4.291(65)	5.875(51)	5.563(30)	3.326(33)	4.488(26)	**3.212(27)**

TABLE 4. THE STATE OF COORDINATION OF CATIONS IN KIRKIITE (cont'd)

Atom **Pb7**, CN: 8, bonded to:

	S11	**S9**	**S7**	**S7**	**S6**	**S6**	**S8**	**S8**
S11	**2.782(58)**	136.0(10)	70.7(11)	70.7(11)	71.2(10)	71.2(10)	132.8(10)	132.8(10)
S9	5.295(60)	**2.928(34)**	73.8(9)	73.8(9)	132.2(8)	132.2(8)	70.5(8)	70.5(8)
S7	3.403(34)	3.612(57)	**3.082(39)**	71.2(13)	140.7(9)	87.4(8)	142.8(9)	89.0(8)
S7	3.403(34)	3.612(57)	3.588(26)	**3.082(39)**	87.4(8)	140.7(9)	89.0(8)	142.8(9)
S6	3.465(53)	5.559(40)	5.870(34)	4.307(39)	**3.151(24)**	89.4(10)	65.6(7)	124.7(7)
S6	3.465(53)	5.559(40)	4.307(39)	5.870(34)	4.431(26)	**3.151(24)**	124.7(7)	65.6(7)
S8	5.492(65)	3.549(29)	5.963(50)	4.411(64)	3.444(49)	5.635(36)	**3.210(31)**	88.7(10)
S8	5.492(65)	3.549(29)	4.411(64)	5.963(50)	5.635(36)	3.444(49)	4.488(26)	**3.210(31)**

Atom **Bi1**, CN: 6, bonded to:

	S2	**S4**	**S3**	**S2**	**S1**	**S3**
S2	**2.478(25)**	92.7(10)	86.0(10)	83.4(12)	83.0(9)	164.4(10)
S4	3.662(48)	**2.583(35)**	91.0(9)	89.1(9)	175.0(8)	85.0(8)
S3	3.492(34)	3.725(52)	**2.640(28)**	169.4(9)	86.4(8)	78.6(10)
S2	3.781(47)	4.048(29)	5.772(42)	**3.157(34)**	92.7(8)	112.0(8)
S1	3.777(38)	5.749(44)	3.998(25)	4.578(57)	**3.171(32)**	98.6(7)
S3	5.696(31)	3.988(32)	3.776(36)	5.329(33)	4.884(37)	**3.271(23)**

Atom **As1**, CN: 6, bonded to:

	S3	**S2**	**S4**	**S1**	**S3**	**S2**
S3	**2.326(45)**	92.4(17)	97.9(17)	92.1(15)	84.8(15)	169.0(19)
S2	3.492(34)	**2.509(43)**	91.4(16)	82.5(14)	176.1(19)	76.5(15)
S4	3.725(52)	3.662(48)	**2.608(60)**	168.6(18)	86.3(14)	82.2(13)
S1	3.998(25)	3.777(38)	5.749(44)	**3.170(55)**	100.3(13)	87.0(12)
S3	3.776(36)	5.696(31)	3.988(32)	4.884(37)	**3.190(43)**	106.2(13)
S2	5.772(42)	3.781(47)	4.048(29)	4.578(57)	5.329(33)	**3.472(47)**

Atom **As2**, CN: 6, bonded to:

	S5	**S8**	**S6**	**S4**	**S3**	**S2**
S5	**2.179(30)**	97.2(12)	94.9(11)	87.8(10)	177.1(11)	82.0(10)
S8	3.326(33)	**2.256(24)**	96.3(11)	83.3(9)	80.3(9)	178.1(10)
S6	3.350(50)	3.444(49)	**2.367(37)**	177.3(9)	84.1(9)	82.1(9)
S4	3.896(37)	3.783(38)	5.679(48)	**3.314(36)**	93.2(7)	98.4(8)
S3	5.603(38)	3.770(40)	3.959(29)	4.897(52)	**3.425(29)**	100.6(7)
S2	3.857(43)	5.758(31)	3.950(32)	5.160(45)	5.329(33)	**3.502(24)**

Atom **As3**, CN: 6, bonded to:

	S9	**S11**	**S10**	**S6**	**S8**	**S5**
S9	**2.174(47)**	106.2(15)	108.0(19)	175.7(12)	74.9(10)	75.0(10)
S11	3.515(60)	**2.221(32)**	109.9(21)	73.9(13)	175.7(14)	71.2(13)
S10	3.62(101)	3.704(67)	**2.302(73)**	75.8(17)	73.3(17)	175.9(19)
S6	5.517(53)	3.465(53)	3.565(64)	**3.346(43)**	104.7(8)	101.1(9)
S8	3.549(29)	5.648(36)	3.541(76)	5.367(49)	**3.431(27)**	105.3(9)
S5	3.598(32)	3.477(59)	5.781(74)	5.273(49)	5.496(33)	**3.482(35)**

The bold numbers in the diagonals are the bond distances (Å), the numbers above the diagonal the bond angles (°), and the numbers below the diagonal the ligand – ligand distances.

layers, and it involves more profound distortions of the structure. A possible composition-plane is (001), with a zig-zag surface. Twinning preserves intact the general anion–cation scheme (*sensu lato*, without regard to the cation species), *e.g.*, their position on $(40\bar{2})$ levels.

An alternative composition-plane, $(20\bar{1})$ can be suggested, with a different mechanism of twinning. The latter includes a slight change in local composition, implying a single incidence of two identical atoms (*e.g.*, a Pb7–Pb7 pair), adjacent to each other along [100]; this mistake displaces the sequences Pb6–Pb7, Pb3–Pb4, and Bi1–Pb1 in the two parts of the twin out of phase by half a period, as required by twinning, and produces the two orientations of the *c* period defined above. This alternative composition-plane is favored by the unpublished observation that, in the original single-crystal work by Moëlo *et al.* (1985), the fragment of the kirkiite crystal was found to have twin lamellae perpendicular to one of the ~8 Å axes.

However, the model of twinning just outlined does not explain the disorder observed by Borodaev *et al.* (1998). For the discussion and interpretation of their

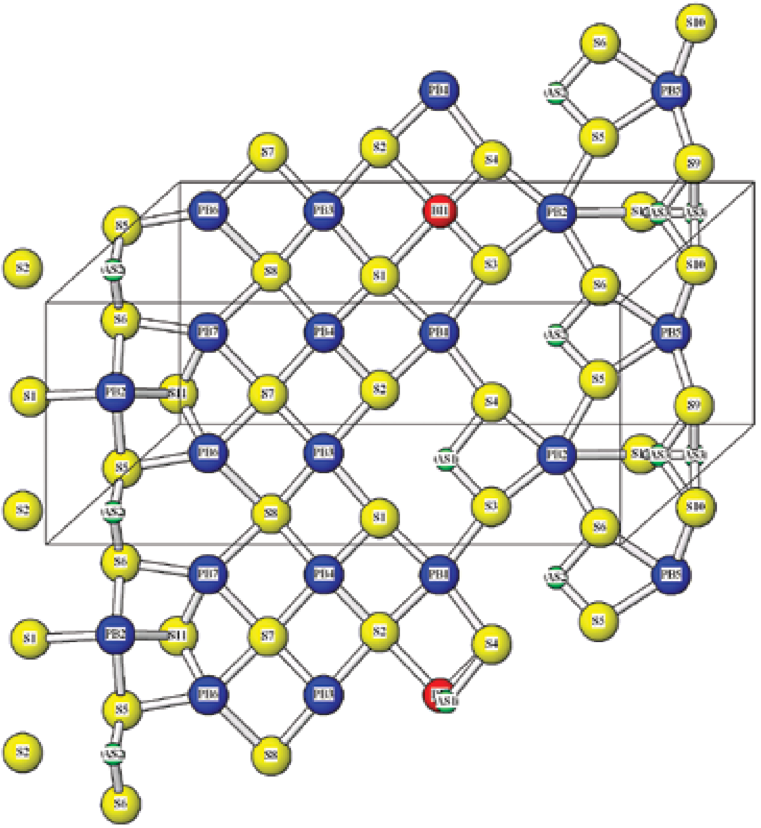

FIG. 4. Surface coordinations for a strongly bonded double layer [approximately (083) of the kirkiite lattice] revealing its trapezoidal character. Pb6 and Pb7 belong to the layer of prisms.

results, a short description of the reciprocal lattice of kirkiite is required. There are three types of reciprocal lattice rows present: (a) Lattice rows with very strong reflections having $k = 8n$, and very few other weak reflections (these almost exclusively for $k = 2n$). These rows define a pseudohexagonal subcell $a'' = b'' = 2.51$ Å and $c'' = 3.26$ Å in the present orientation. (b) Lattice rows of strong reflections without extinctions; they are situated in the center of each triangular interspace of the previous reciprocal lattice. Together with the previous system of rows, they define a subcell with $a' = c' = 4.35$ Å and $b' = b_{\text{cell}}$, rotated 30° with respect to the previous one. (c) Lattice rows, parallel to b^*_{cell} of weak reflections halving all the distances between any two adjacent rows of the two previous systems combined. No extinctions were observed for these rows; they are underlain by weak streaking and occasionally contain reflections halving the b^*_{cell} period of 1/26 Å. These spurious reflections were found on several, commonly adjacent rows of the reciprocal lattice of the (c) category, without any systematic distribution in reciprocal space. Their non-systematic occurrence is, perhaps, due to twinning of the grain examined. Thus, no unambiguous interpretation can be given for these additional reflections, similar to the "*C* centering" of Borodaev *et al.* (1998), when we use our notation for the 26 Å axis. It is the rows of the (c) category that were converted into pure streaks or exhibited the infrequently occurring "centering" reflections in the work of Borodaev *et al.* (1998).

The structural model for the disorder along *b* in kirkiite has to preserve the substructures (a) and (b) (*i.e.*, the generalized cation–anion scheme) intact and involve only the reflections of the (c) rows, *i.e.*, the structural details. It means that the distinct polytypes of kirkiite present in different proportions in the specimens with (c) rows converted into streaks or containing patterns of reflections different from the model described above are created by an exchange of atomic species in some of the generalized positions of the cations.

A model proposed for the centered $b = 2 \times 26$ Å polytype observed by Borodaev *et al.* (1998) and supported by the rare "additional" reflections in the present sample, also represents twinning $1\,0\,0 / 0\,\bar{1}\,0 / 1\,0\,\bar{1}$, but the contact plane is the median plane of the layer (010) of prisms in the structure, instead of the previously suggested planes. The suggested mechanism of polytype formation is the system of two-fold axes [102] in this layer, acting on the adjacent layers of octahedra, *i.e.*, layer stacks in the new polytype. These two-fold axes replace the reflection plane (010), which is active in the untwinned structure. In the latter, Pb4 of the adjacent layer of octahedra is reflected into Pb4 on the other side of prismatic layer, and this is true for the entire cation-configurations of stacks of adjacent layers. Inspection of Figure 3 shows, especially on the example of As3–As3' pairs, how the configurations in the layers of prisms, situated at ±½ *b* on both sides of the central *m* plane in question, assume a position by 1/4 [100] "higher" than on the mirror plane, the action of which we examine. Replacing the active *m* by a 2-fold axis, the left-hand position of the As3–As3' pair will be by 1/4 [100] lower than the "central" one, and the resulting pattern of occupancy will give a *C*-centered rectangular cell, but with monoclinic symmetry.

The latter structure is not a true OD structure, although it can be approximated by an OD structure composed of two kinds of layers. This can be seen by considering cation positions in the layer of prisms in which the twinning takes place. In the untwinned structure, the topologically equivalent rows [001] and [101] are occupied by partly mixed Pb6 sites and by fully lead-occupied Pb7 sites, respectively (Fig. 2c). The opposite is true for the first layer of octahedra, *etc.* The formation of an alternative polytype will probably be connected with the occupation of Pb5–Pb7 and Pb5–Pb6 rows by basically the same mix of cation species. This cation disorder might alter the β angle locally to ~120°, facilitating the "loss of orientation memory" for the stacks of octahedra when proceeding from one side of the prismatic boundary to its opposite side, and leading to the creation of the structural disorder observed by Borodaev *et al.* (1998).

TABLE 5. COORDINATION NUMBERS AND SELECTED POLYHEDRON-DISTORTION PARAMETERS

Site	CN	1	2	3	4	5	6	7
Pb1	6	3.004	3.023	115.68	0.235	0.065	34.42	1.94
Pb2	6	3.018	3.028	116.32	0.262	0.074	34.28	1.99
Bi1	6	2.883	2.974	110.17	0.513	0.123	30.74	3.44
As1	6	2.879	2.974	110.17	0.618	0.123	30.74	1.94
As2	6	2.841	3.017	115.01	0.763	0.187	29.75	3.14
As3	6	2.826	3.107	125.62	0.864	0.351	25.95	3.40
Pb3	7	3.032	3.036	117.20	0.164	0.066	41.45	2.00
[Pb,Bi]4	7	3.000	3.000	113.11	0.232	0.059	40.30	2.26
Pb5	8	3.135	3.111	126.15	0.224	0.049	52.00	2.00
[Pb,Bi]6	8	3.019	3.037	117.31	0.206	0.061	47.76	2.51
Pb7	8	3.074	3.086	123.11	0.140	0.059	50.21	2.10

CN: coordination number. Column headings: 1: Average bond-distance (Å), 2: Radius of circumscribed sphere (Å), 3: Sphere volume, V_s (Å^3), 4: Volume eccentricity, Δ, 5: Volume distortion, ν, 6: Polyhedron volume, V_p (Å^3), 7: Valence sum (*vu*, valence units).
The parameters of atom coordinations are defined in Balić-Žunić & Makovicky (1996) and Makovicky & Balić-Žunić (1998), except for the bond valence, defined as in Brown & Altermatt (1985), with bond-valence parameters of Brese & O'Keeffe (1991). All calculations done with the program IVTON (Balić-Žunić & Vicković 1996).

The crystal structure of kirkiite is formed by unit-cell twinning, on planes of prisms, of a stack ABC of slabs of octahedra, with some distortions arising primarily from the accommodation of pairs of lone electrons. Therefore, the configurations along the [100] rows are very similar to those on [001] rows, and incompletely matched also by those on [101] rows in all layers. All the twinning phenomena described could, with somewhat diminished probability, happen for the second orientation, whereas this type of polytype building does not exist for the third orientation, Pb5 and Pb7 being pure Pb positions (Fig. 2c). In the third orientation, twinning would mean that the quasi-mirror plane has been replaced by a true mirror, interchanging the unequal *a* and *c* axes by its action. The splitting of reflections created by this type of twinning was not observed in the sample studied.

CONCLUDING REMARKS

Kirkiite has a highly pseudosymmetric structure, overloaded with heavy atoms and prone to multiple twinning. In the light of this, the current results of the structure determination can be considered satisfactory. Some of the features quoted by Ito & Nowacki (1974) for the crystal structure of jordanite (*e.g.*, mixed positions Pb–As) can perhaps be ascribed to similar twinning-based phenomena.

ACKNOWLEDGEMENTS

This project was supported by the grant no. 9901772 of the National Research Council (Natural Science) of Denmark, and by the Ministry of Science and Environmental Protection of the Republic of Serbia. Keen interest of Dr. S. Karup-Møller (Lyngby) as well as the valuable remarks by Dr. Y. Moëlo (Nantes), Prof. F. Vurro (Bari) and the assistance of Mrs. C. Sarantaris are appreciated.

REFERENCES

BALIĆ-ŽUNIĆ, T. & MAKOVICKY, E. (1996): Determination of the centroid or 'the best centre' of a coordination polyhedron. *Acta Cristallogr.* **B52**, 78-81.

BALIĆ-ŽUNIĆ, T. & VICKOVIĆ, I. (1996): *IVTON* – a program for the calculation of geometrical acpects of crystal structures and some crystal chemical applications. *J. Appl. Crystallogr.* **29**, 305-306.

BORODAEV, Y.S., GARAVELLI A., KUZMINA, O.V., MOZGOVA, N.N., ORGANOVA, N.I., TRUBKIN, N. & VURRO, F. (1998): Rare sulfosalts from Vulcano, Aeolian islands, Italy. I. Se-bearing kirkiite, $Pb_{10}(Bi,As)_6(S,Se)_{19}$. *Can. Mineral.* **36**, 1105-1114.

BRESE, N.E. & O'KEEFFE, M. (1991): Bond valence parameters for solids. *Acta Crystallogr.* **B47**, 192-197.

BROWN, I.D. & ALTERMATT, D. (1985): Bond valence parameters obtained from a systematic analysis of the Inorganic Crystal Structure Database. *Acta Crystallogr.* **B41**, 244-247.

ĎUROVIČ, S. (2004): Layer stacking in general polytypic structures. *In* International Tables for Crystallography, Vol. C., Sect. 9.2 (3rd ed.). Kluwer Acad. Publ., Dordrecht, The Netherlands.

ITO, T. & NOWACKI, W. (1974): The crystal structure of jordanite, $Pb_{28}As_{12}S_{46}$. *Z. Kristallogr.* **139**, 161-185.

MAKOVICKY, E. (1989): Modular classification of sulphosalts – current status. Definition and application of homologous series. *Neues Jahrb. Mineral., Abh.* **160**, 269-297.

MAKOVICKY, E. & BALIĆ-ŽUNIĆ, T. (1998): New measure of distortion for coordination polyhedra. *Acta Cristallogr.* **B54**, 766-773.

MOËLO, Y., OUDIN, E., MAKOVICKY, E., KARUP-MØLLER, S., PILLARD, F., BORNUAT, M. & EVANGHELOU, E. (1985): La kirkiite, $Pb_{10}Bi_3As_3S_{19}$, une nouvelle espèce minérale homologue de la jordanite. *Bull. Minéral.* **108**, 667-677.

SHELDRICK, G.M. (1997a): *SHELXS97. Program for the Solution of Crystal Structures.* University of Göttingen, Göttingen, Germany.

SHELDRICK, G.M. (1997b): *SHELXL97. Program for the Refinement of Crystal Structures.* University of Göttingen, Göttingen, Germany.

WALIA, D.S. & CHANG, L.L.Y. (1973): Investigation in the systems $PbS–Sb_2S_3–As_2S_3$ and $PbS–Bi_2S_3–As_2S_3$. *Can. Mineral.* **12**, 113-119.

WUENSCH, B.J. & NOWACKI, W. (1966): The substructure of the sulfosalt jordanite, *Schweiz. Mineral. Petrogr. Mitt.* **46**, 89-96.

Received February 6, 2004, revised manuscript accepted January 2, 2006.